

Features of planar metal/dielectric nanowaveguides

V.M. Fitio¹, A.V. Bendziak¹, I.Ya. Yaremchuk¹, Ya.V. Bobitski^{1,2}

¹*Department of Photonics, Lviv Polytechnic National University,
Bandera str. 12, 79013 Lviv, Ukraine,*

²*College of Natural Sciences, University of Rzeszow*

Pigonia Str.1, 35310 Rzeszow, Poland

E-mail: v.m.fitio@gmail.com

Abstract. Results of analysis focused on dielectric/metal/dielectric and metal/dielectric/metal symmetric nanowaveguides have been presented. The waveguides based on gold, silver and aluminum have been studied. It has been shown that silver as metal is the most suitable to be used in metal/dielectric/metal waveguide from the viewpoint waveguide thickness minimization and the minimal absorption under optical wave propagation.

Keywords: waveguide, noble metal, dielectric, propagation constant, field penetration depth.

<https://doi.org/10.15407/spqeo23.02.168>

PACS 42.25 Bs, 42.25 Hz, 42.79 Ci

Manuscript received 23.05.19; revised version received 23.03.20; accepted for publication 10.06.20; published online 12.06.20.

1. Introduction

Recently, interest in such field of optics as plasmonics [1, 2] has increased. A lot of different plasmonic elements and devices are developed on their base. Among them the nanolasers, the so-called “Spasers”, cause a huge interest [3, 4], as well as nanolasers in the ultraviolet range on the basis of aluminum [5]. Moreover, devices in which the plasmon effects are implemented for practical application, in particular for the analysis of biochemical media on the basis of resonance absorption of a surface plasmon-polariton wave [6-8] are now under intense researching.

It is possible to develop the integrated optical circuits based on the nanolasers and amplifying nanostructures (analogous of transistor in traditional electronics). They are the base for an optical processor that can operate in the terahertz range as predicted.

It is necessary to create the waveguides connecting active optical elements that can support propagating radiation and are analogous to metal conductors in the traditional processors. Absorption of the optical wave can be allowed in the waveguides, since the distances between active elements are short in these optical integrated circuits. The analysis of dielectric/dielectric/dielectric planar waveguides shows that they do not provide a strong localization of the field. Thus, they should have the

thickness of several micrometers [9], which is not quite acceptable. At the same time, waveguides based on propagation of the surface plasmon-polariton wave in the metal/dielectric/metal or dielectric/metal/dielectric structures can have a small thickness, especially the structure of the first type [2]. The periodic repetition of the metal/dielectric/metal structure is realized in the grating that is characterized by the abnormal high transmission. It is a result of the occurrence of waveguide mode in the dielectric slit at subwavelength thicknesses of the dielectric layer [10, 11]. The waveguide mode with low losses arises due to the surface plasmon-polariton wave, which propagates along the metal-dielectric interface [2].

The absorption of metal defines the energy loss of the propagation modes in the waveguide, if the absorption in dielectrics is taken as negligible in analysis. Absorption in the metal is defined by the imaginary part of the dielectric constant. Therefore, we analyzed the waveguides with silver, gold and aluminum metals, which have relatively small imaginary parts of the dielectric function [12-14].

The approximate analytical dependences in the range of wavelengths from 0.3 up to 2.0 μm for gold and silver, from 0.3 up to 4.0 μm for copper and from 0.1 up to 2.0 μm for aluminum were found on the base of experimentally measured spectral dependences of

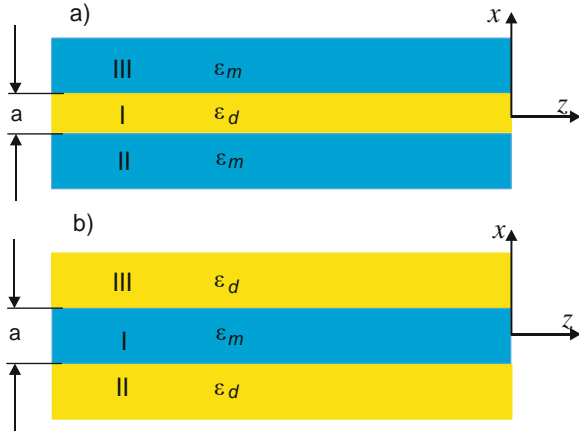


Fig. 1. Schemes of waveguides: metal/dielectric/metal structures (a), dielectric/metal/dielectric structures (b), where a is the thickness of the middle waveguide layer, ε_m is the dielectric permittivity of metal, ε_d is the dielectric permittivity of dielectric.

dielectric permittivity of these metals [15]. These analytic dependences were used to calculate the propagation constant of the waveguides shown in Fig. 1.

In this paper, we study propagation of the transverse magnetic (TM) polarized wave, for which the magnetic field vector is parallel to the metal/dielectric boundary. Propagation of the surface plasmon-polariton wave is possible only for this polarization. The propagation constant of the waveguides is different from that of the plasma-polariton wave near the metal/dielectric boundary, since the metal or dielectric layer is limited in thickness in both types of waveguides, and it will be confirmed by numerical experiments.

2. Theoretical background

In a general case, the electric field intensity of the propagating wave of TM polarization can be written as follows:

$$\mathbf{E}(x, z) = [\mathbf{e}_x E_x(x) + \mathbf{e}_z E_z(x)] \exp(i\beta z),$$

where \mathbf{e}_x , \mathbf{e}_z are the unit vectors directed along the axes x and z ; $E_x(x)$, $E_z(x)$ are projections of the electric field intensity, on the x and z axes, respectively; β is the propagation constant of the electromagnetic wave in the waveguide.

Modern software allows to simply find the propagation constant of the waveguides shown in Fig. 1. Let use analytical expressions [2, 7] and modify them. The propagation constant can be written as follows:

$$\beta = \text{Re}\beta + i\text{Im}\beta.$$

Knowing the imaginary part of the dielectric constant, the distance L on which the field intensity decreases by $e \approx 2.718$ times in accordance with the expression $L = 1/\text{Im}\beta$ can be determined.

The projections of wave vectors on the x -axis for three waveguide layers can be written as follows:

$$k_j^2 = \beta^2 - k_0^2 \varepsilon_j, \text{ where } j = 1, 2, 3; k_0 = \frac{2\pi}{\lambda}.$$

In a general case, the dispersion equation, from which the propagation constants β are determined, will have the form [2]:

$$D(\beta) = \exp(-4k_1 a) = \frac{\frac{k_1 + k_2}{\varepsilon_1} + \frac{k_1 + k_3}{\varepsilon_2}}{\frac{k_1 - k_2}{\varepsilon_1} - \frac{k_1 - k_3}{\varepsilon_2}} \times \frac{\frac{k_1 + k_3}{\varepsilon_1} + \frac{k_1 + k_2}{\varepsilon_3}}{\frac{k_1 - k_3}{\varepsilon_1} - \frac{k_1 - k_2}{\varepsilon_3}} = 0. \quad (1)$$

In case of a symmetric waveguide, $\varepsilon_2 = \varepsilon_3$ and $k_2 = k_3$. Therefore, dispersion equation (1) can be separated by two equations in the following way:

$$D(\beta) = \text{th}(k_1 a/2) = \frac{k_2 \varepsilon_1}{k_1 \varepsilon_2} = 0, \quad (2)$$

$$D(\beta) = \text{th}(k_1 a/2) = \frac{k_1 \varepsilon_2}{k_2 \varepsilon_1} = 0. \quad (3)$$

The first equation defines the mode for which $E_z(x)$ is an odd function, and $E_x(x)$ is a pair function. The equations (2) define the mode for which $E_z(x)$ is a pair function, and $E_x(x)$ is the odd function. For the waveguide shown in Fig. 1a, $\varepsilon_2 = \varepsilon_d$, $\varepsilon_1 = \varepsilon_m$ and for the waveguide shown in Fig. 1b, $\varepsilon_2 = \varepsilon_m$, $\varepsilon_1 = \varepsilon_d$.

It is evident that $D(\beta)$ is a complex function, and it can be equal to zero under condition that the real and imaginary parts of $D(\beta)$ are also equal to zero. There are the two implicitly given functions $\text{Re}[D(\text{Re}\beta + i\text{Im}\beta)] = 0$, $\text{Im}[D(\text{Re}\beta + i\text{Im}\beta)] = 0$. Thus, crossing of curves $\text{Re}[D(\text{Re}\beta + i\text{Im}\beta)] = 0$, $\text{Im}[D(\text{Re}\beta + i\text{Im}\beta)] = 0$ in the coordinate system $\text{Re}\beta$, $i\text{Im}\beta$ determines the propagation constants $\beta = \text{Re}\beta + i\text{Im}\beta$. This task is effectively solved for a short-time interval using modern programming tools. It should be noted that the $\text{th}(k_1 a/2)$ function is used in the equations (2) and (3). It is due to the fact that in the layer I, whether it is metallic or dielectric, the field intensity decreases according to the exponential law, if moving from the metal/dielectric boundary, which is typical for the plasmon-polariton wave propagation.

The $\text{th}(k_1 a/2)$ function turns into $\tan(k_1 a/2)$ function, if planar waveguide is totally dielectric. When the dispersion equations from the ref. [7] are used, then to find propagation constant for the above presented waveguides, it is necessary to replace $\sin(k_1 a/2)$ and $\cos(k_1 a/2)$ by $\sinh(k_1 a/2)$ and $\cosh(k_1 a/2)$, respectively.

The spectral dependences of the dielectric permittivities of gold, silver and aluminum for the wavelength range from 0.3 to 2 μm are presented in Fig. 2.

These dependences are based on the works [12-14]. It can be seen that the imaginary and real parts of dielectric permittivity of gold and silver within the range of wavelengths from 0.6 to 1.2 μm are quite close. The imaginary parts of the aluminum dielectric permittivity in the ultraviolet region are quite low, and the real part of the dielectric permittivity is negative.

As a result, surface plasmon-polariton wave propagation at the boundary of the aluminum/dielectric in the ultraviolet region of the spectrum is possible [16]. The surface plasmon-polariton waves cannot propagate in the ultraviolet region for gold and silver, since $\text{Re}(\epsilon)$ is either positive (silver) or very small in modulus (gold), but negative (see Fig. 2).

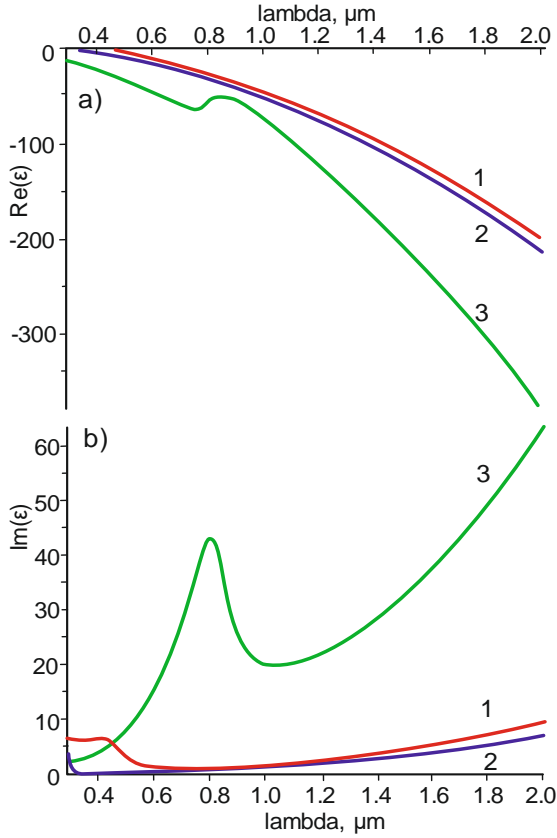


Fig. 2. Spectral dependence of the dielectric permittivity of gold (1), silver (2), aluminum (3); (a) the real part of dielectric permittivity, (b) the imaginary part of dielectric permittivity.

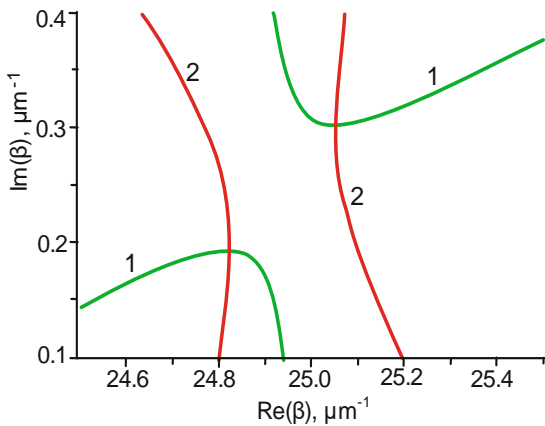


Fig. 3. Solution of the dispersion equation with the following data: metal is aluminum, $a = 0.05 \mu\text{m}$, $\epsilon_d = 2.25$, $\lambda = 0.4 \mu\text{m}$, $\text{Re}[D(\beta)] = 0$ represented by the curves 1, $\text{Im}[D(\beta)] = 0$ shown by the curves 2.

3. Theoretical results and discussion

In the first step, let us consider the dielectric/metal/dielectric waveguide shown in Fig. 1b. The two modes – the pair (symmetric) and odd (antisymmetric) – can be found using the dispersion equations from [7]. The solution of dispersion equation is shown in Fig. 3. Used in all the calculations is $\epsilon_d = 2.25$. The curves 1 and 2 intersect practically at the right angle. Therefore, using the standard software, one can determine the coordinates of intersection for these curves, at least with four significant digits. In our case, they are equal $\beta_{as} = 24.82 + i0.1926 \mu\text{m}^{-1}$, $\beta_s = 25.05 + i0.3013 \mu\text{m}^{-1}$ for the antisymmetric and symmetric modes, respectively.

In addition, propagation constants were determined using the equations (2) and (3). The results of the calculations were identical. The antisymmetric mode has significantly less absorption, which is defined by $\text{Im}\beta$, as compared to the symmetric mode.

The dependences of the propagation constants for this waveguide on the thickness of the layer of aluminum for the wavelength $0.4 \mu\text{m}$ are shown in Fig. 4. Analyzing Fig. 4, it can be concluded that propagation constants of

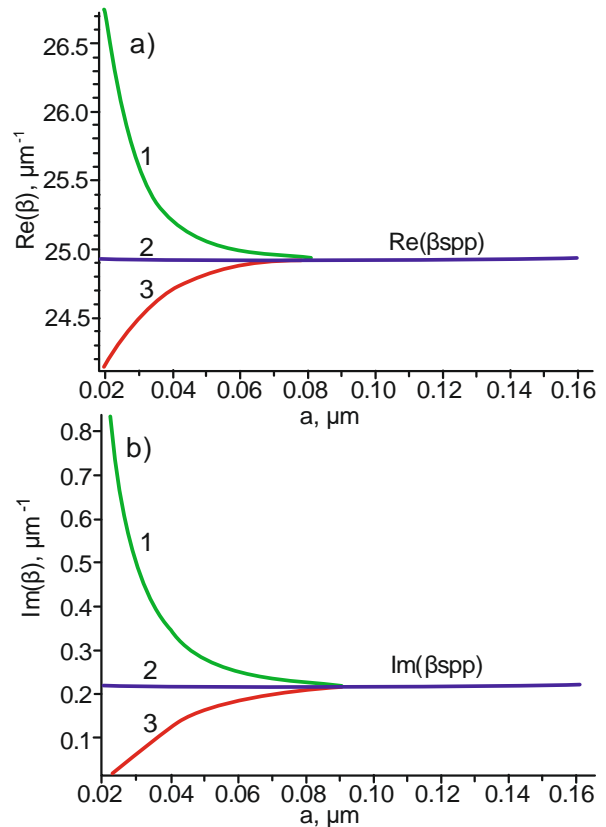


Fig. 4. Dependences of the propagation constants in the dielectric/metal/dielectric waveguide on the thickness of metal: a) the real part of propagation constants, b) the imaginary part of propagation constants. Aluminum is used as metal, $\epsilon_d = 2.25$, $\lambda = 0.4 \mu\text{m}$. The symmetric mode is represented by the curves 1, antisymmetric mode is represented by the curves 3, the propagation constant of the surface plasmon-polariton wave at the metal/dielectric boundary is represented by the curves 2.

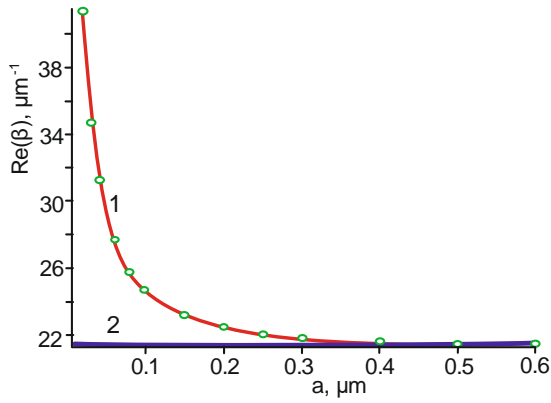


Fig. 5. Dependence of the real part of propagation constant on the thickness of dielectric layer a for the waveguide according to Fig. 1a with silver at the wavelength $0.5 \mu\text{m}$; the calculation carried out according to the dispersion equation from the book [7] is represented by the curve 1, the calculation carried out by the method from [11] is represented by the circles, the curve 2 represents the real part of constant propagation of the surface plasmon-polariton wave at the metal/dielectric boundary.

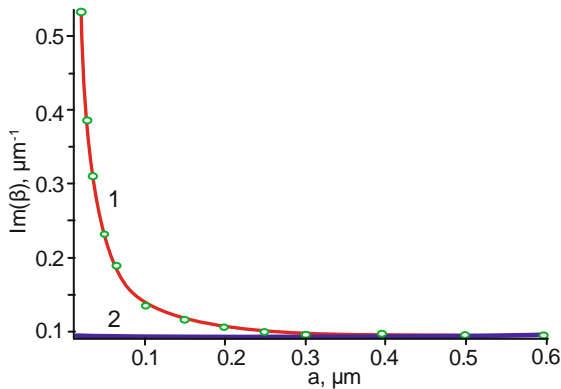


Fig. 6. Dependences of the imaginary part of propagation constant on the thickness of dielectric layer a for the waveguide according to Fig. 1a with silver at the wavelength $0.5 \mu\text{m}$. The curve 1 represents the calculation carried out according to the dispersion relation of the book [7], the circles represent the calculation by using the method of work [11], and the straight line 2 shows the imaginary part of propagation constant for the surface plasmon-polariton wave at the metal/dielectric boundary.

both modes with increasing thickness of the metal film approach to the propagation constant β_{spp} of the surface plasmon-polariton wave. It can be supposed on the base of the relation $k_x = \sqrt{k_0^2 \epsilon_d - \beta^2}$ that when the thickness of the metal decreases, the field penetrates deeper into the dielectric for the antisymmetric mode.

Therefore, this waveguide will have a large thickness for significant localization of the power in the propagation mode inside the waveguide. The absorption in the waveguide increases significantly when the thickness of the metal layer decreases for the symmetrical mode. This mode has better localization of the field. These findings are also valid for such metals as gold and silver.

However, it should be expected that the metal/dielectric/metal waveguide will have better localization of the field in the waveguide according to the ratio $k_x = \sqrt{k_0^2 \epsilon_m - \beta^2}$. Since the real part of the dielectric permittivity of metal is negative. Therefore, the properties of the waveguide shown in Fig. 1a should be examined in more detail.

The calculation of propagation constants was carried out according to Eqs (2) and (3), dispersion equation from the book [7], and also according to the method described in [11]. All three methods give the same numerical values of propagation constant for this waveguide. This propagation constant has been determined by surface plasmon-polariton waves at the metal/dielectric boundary. The anomalous high transmission by the metal grating with narrow dielectric slit can be explained with account of this propagation constant [10, 11].

The dependence of the real part of propagation constant on the thickness of dielectric layer in the waveguide with silver for the wavelength $0.5 \mu\text{m}$ is shown in Fig. 5.

According to this figure, the real part of propagation constant monotonically increases, when the thickness of dielectric layer decreases. This property is valid for all other parameters for the waveguide shown in Fig. 1a, thus the corresponding curves are typical.

The dependence of the imaginary part of propagation constant on the thickness of dielectric layer in the waveguide with silver for the wavelength $0.5 \mu\text{m}$ is shown in Fig. 6.

The dependences of the imaginary part of propagation constant on the thickness of dielectric layer in the waveguide with aluminum for the wavelength $0.4 \mu\text{m}$ are shown in Fig. 7.

It can be concluded analyzing Fig. 7 that there is such a thickness of the dielectric layer that the imaginary part of the dielectric constant is minimal. In this case, the thickness is equal to $0.4 \mu\text{m}$.

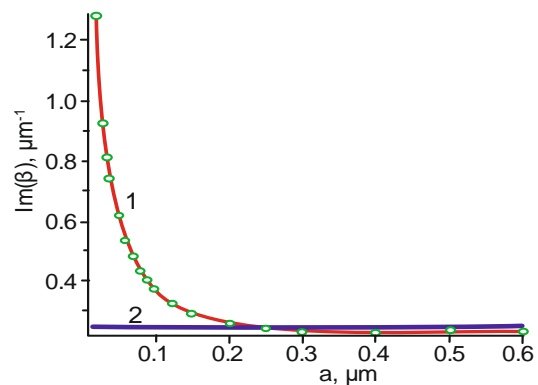


Fig. 7. Dependences of the imaginary part of propagation constant on the thickness of dielectric layer a for the waveguide according to Fig. 1a from aluminum at the wavelength $0.4 \mu\text{m}$. The curve 1 represents the calculation carried out according to the dispersion relation of the book [7], the circles represent the calculation by using the method from work [11], and straight line 2 represents the imaginary part of propagation constant of the surface plasmon-polariton wave at the metal/dielectric boundary.

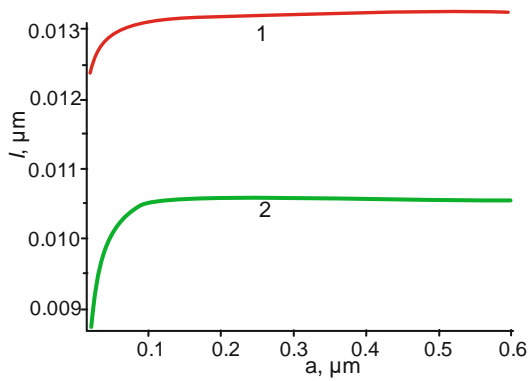


Fig. 8. Dependences of the depth of field penetration into metal on the thickness of dielectric layer. 1 – the wavelength 0.4 μm, 2 – the wavelength 0.2 μm.

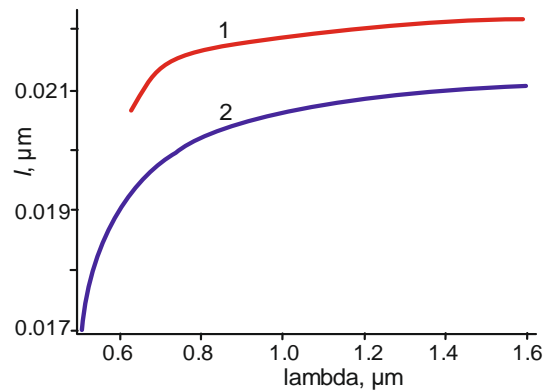


Fig. 11. Dependences of the depth of field penetration into metal of waveguide on the wavelength at $a = 0.02 \mu\text{m}$ for gold (1) and silver (2).

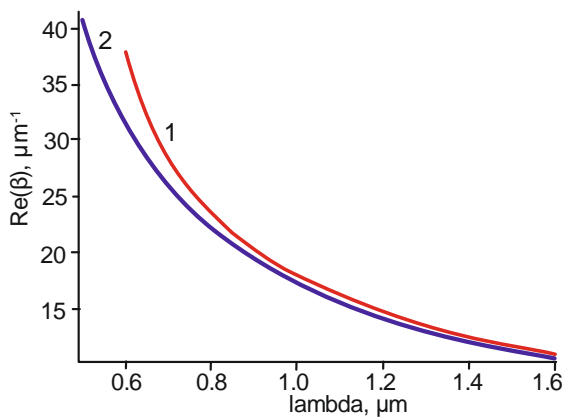


Fig. 9. Dependences of the real part of propagation constant on the wavelength at $a = 0.02 \mu\text{m}$ for the waveguide according to Fig. 1a. The curve 1 corresponds to gold, and curve 2 – to silver.

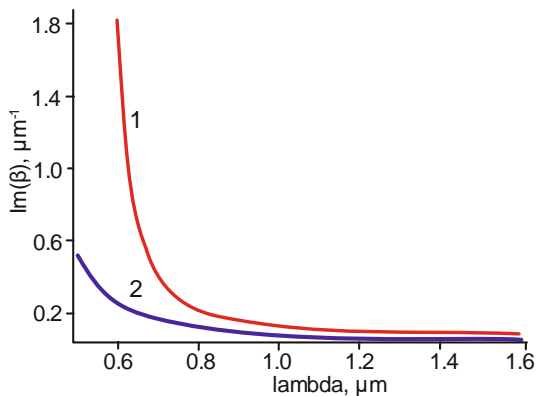


Fig. 10. Dependence of the imaginary part of propagation constant on the wavelength at $a = 0.02 \mu\text{m}$ for the waveguide according to Fig. 1a. The curve 1 corresponds to gold, and curve 2 – to silver.

The depth of penetration of the electromagnetic field into the metal layer is an important characteristic of this waveguide. The dependence of penetration of the electromagnetic field into metal is shown in Fig. 8.

In fact, the depth of field penetration into the outer layers of the waveguide, in this case metal, defines the thickness of waveguide. It is evident that the waveguide should be the nanowaveguide, if the depth of field penetration is small. The depth of penetration is determined from the following expression:

$$l = \frac{1}{\text{Im}(k_x)}, \quad (4)$$

where $k_x = \sqrt{k_0^2 \varepsilon_m - \beta^2}$.

The dependences of field penetration into aluminum on the thickness of dielectric layer for the wavelengths 0.4 and 0.2 μm are shown in Fig. 8.

The depth of field penetration in aluminum is rather small, and it is practically constant in a wide range of changes in the thickness of dielectric layer. It decreases with decreasing the layer thickness, when the thickness of dielectric layer is less than 0.1 μm.

The dependences of real part of the waveguide propagation constant on the wavelength at $a = 0.02 \mu\text{m}$ for gold and silver are shown in Fig. 9.

The real parts of propagation constants for two waveguides are very close to each other at the wavelengths longer than 1.0 μm. To some extent, it is explained by Fig. 2. The dependences of imaginary part of the waveguide propagation constant on the wavelength at $a = 0.02 \mu\text{m}$ for gold and silver are shown in Fig. 10.

The imaginary part of dielectric constant is larger for gold than for silver in the given range of wavelengths (see Fig. 10). It coincides with the data of Fig. 2. Moreover, the imaginary part of propagation constant at the wavelengths longer than 1 μm is less than $0.2 \mu\text{m}^{-1}$. It means that the amplitude of field decreases by $e \approx 2.718$ times at spreading by 5 μm in the waveguide.

The dependences of field penetration depth into metal of waveguide on the wavelength for $a = 0.02 \mu\text{m}$ for gold and silver are shown in Fig. 11. It can be concluded from Fig. 11 that the depth of field penetration into metal for silver is less than for gold, but they are quite close to each other. In addition, it can be observed an interesting feature, if considering Figs 8 to 10. The

curves 2 (gold) are in the narrower range of wavelengths (from 0.63 to 1.6 μm) than silver (from 0.5 to 1.6 μm). This can be explained by the fact that the calculated field penetration depth, according to the equation (4), is negative at the wavelengths less than 0.63 μm . Therefore, waveguide effect cannot be physically realized at these wavelengths. Although, from the mathematical viewpoint, using the equation (2) is acceptable.

3. Conclusion

Two types of waveguides metal/dielectric/metal and dielectric/metal/dielectric have been analyzed. Weak localization of the field inside the metal layer is characteristic for the second waveguide. Here, the field penetrates to the considerable depth into the dielectric. Therefore, the dielectric/metal/dielectric waveguide is not suitable for creation of the nanowaveguide for optical integrated circuits. The first type waveguide provides strong localization of the field into the waveguide, since the depth of field penetration into the metal is 10...13 nm for aluminum and 19...22 nm for silver and gold. The total thickness of the waveguide should be 100 nm, if using the thickness of metal layers close to 40 nm and the thickness of dielectric layer 20 nm in this waveguide, and it is quite acceptable for the integrated optical circuits.

Acknowledgements

The work was supported by Ministry of Education and Science of Ukraine (grant DB/Interface No 0120U100675, DB/MEV No 0118U000267).

References

1. Stockman M. I., Kneipp K., Bozhevolnyi S.I., Saha S., Dutta A., Ndukaife J., & Boltasseva A. Roadmap on plasmonics. *J. Opt.* 2018. **20**, No 4. P. 043001. <https://iopscience.iop.org/article/10.1088/2040-8986/aa114>.
2. Maier S., *Plasmonics: Fundamentals and Applications*. Springer, 2007. https://link.springer.com/chapter/10.1007%2F0-387-37825-1_2.
3. Ye Y., Liu F., Cui K., Feng X., Zhang W. & Huang Y. Free electrons excited SPASER. *Opt. Exp.* 2018. **26**, No 24. P. 31402–31412. <https://www.osapublishing.org/oe/abstract.cfm?uri=oe-26-24-31402>.
4. Pei Song, Jian-Hua Wang, Miao Zhang, Fan Yang, Hai-Jie Lu, Bin Kang, Jing-Juan Xu, Hong-Yuan Chen Three-level spaser for next-generation luminescent nanoprobe. *Science Adv.* 2018. **4**, No 8. P. eaat0292. <https://advances.sciencemag.org/content/4/8/eaat0292?rss=1>.
5. Zhang Q., Li G., Liu X., Qian F., Li Y., Sum T.C., Lieber C.M., Xiong Q. A room temperature low-threshold ultraviolet plasmonic nanolaser. *Nature Commun.* 2017. **5**. P. 4953. <https://www.nature.com/articles/ncomms5953>.
6. Yaremchuk I., Petrovska H., Fitio V., Bobitski Y. Optimization and fabrication of the gold-coated GaAs diffraction gratings for surface plasmon resonance sensors. *Optik.* 2018. **158**. P. 535–540. <https://www.sciencedirect.com/science/article/pii/S030402617317862>.
7. Unger H.-G. Planar Optical Waveguides. In: Ostrowsky D.B. (eds) *Fiber and Integrated Optics*. NATO Advanced Study Institutes Series (Series B: Physics). 1979. **41**. P. 183–221. Springer, Boston, MA. https://doi.org/10.1007/978-1-4613-2937-4_9.
8. Lesyuk R., Klein E., Yaremchuk I., Klinke C. Copper sulfide nanosheets with shape-tunable plasmonic properties in the NIR region. *Nanoscale.* 2018. **10**, No 44. P. 20640–20651. <https://pubs.rsc.org/en/content/articlehtml/2018/nr/c8nr06738d>.
9. Selvaraja S.K., Sethi P. Review on optical waveguides. In: *Emerging Waveguide Technology*. IntechOpen, 2018. <https://www.intechopen.com/books/emerging-waveguide-technology/review-on-optical-waveguides>.
10. Liang Y., Peng W., Hu R., Xie L. Extraordinary optical properties in the subwavelength metallo-dielectric free-standing grating. *Opt. Exp.* 2014. **22**, No 16. P. 19484–19494. <https://www.osapublishing.org/oe/abstract.cfm?uri=oe-22-16-19484>.
11. Fitio V.M. Transmissions of metallic gratings with narrow slots. *Proc. LFNM 2006, 8th Intern. Conf. on Laser and Fiber-Optical Networks Modeling*, 2006, P. 113–116. <https://ieeexplore.ieee.org/abstract/document/4018215>.
12. McPeak K.M., Jayanti S.V., Kress S.J.P., Meyer S., Iotti S., Rossinelli A., Norris D.J. Plasmonic films can easily be better: Rules and recipes. *ACS Photonics.* 2015. **2**. P. 326–333. <https://pubs.acs.org/doi/abs/10.1021/ph5004237>.
13. Babar S., Weaver J.H. Optical constants of Cu, Ag, and Au revisited. *Appl. Opt.* 2015. **54**. P. 477–481. <https://www.osapublishing.org/ao/abstract.cfm?uri=ao-54-3-477>.
14. Yakubovsky D.I., Arsenin A.V., Stebunov Y.V., Fedyanin D.Y., Volkov V.S. Optical constants and structural properties of thin gold films. *Opt. Exp.* 2017. **25**, No 21. P. 25574–25587. <https://www.osapublishing.org/oe/abstract.cfm?uri=oe-25-21-25574>.
15. Fitio V., Vernygor O., Yaremchuk I., Bobitski Y. Analytical approximations of the noble metals dielectric permittivity. *14th Intern. Conf. on Advanced Trends in Radioelectronics, Telecommunications & Computer Engineering (TCSET)*, 2018, February 20-24, Lviv–Slavske, Ukraine. P. 426–430. <https://ieeexplore.ieee.org/abstract/document/8336233>.
16. Fu X., Ren F., Sun S., Tian Y., Wu Y., Lou P. High-sensitivity nanostructured aluminium ultrathin film sensors with spectral response from ultraviolet to near-infrared. *Physica Scripta.* 2019. **94**. P. 055504. <https://iopscience.iop.org/article/10.1088/1402-4896/ab0a12>.

Authors and CV



Volodymyr M. Fitio, born in 1950, defended his Doctoral Thesis in Physics and Mathematics in 2009 and became full professor in 2017. Professor at the Department of Photonics, Lviv Polytechnic National University. Authored over 200 publications. The area

of his scientific interests includes holography, diffraction by periodical and chaotic structures, distribution light by waveguide, feedback lasers and the application of numerical methods for the analysis and design of optic elements and devices.



Andrii V. Bendziak, born in 1993, defended his Master degree in 2015. Working as young scientific researcher at the Department of Photonics, Lviv Polytechnic National University. The area of his scientific interest includes diffraction by periodical structures, numerical methods

for the analysis of light distribution in multilayer waveguides and periodical structures.



Iryna Ya. Yaremchuk, born in 1980, defended her Doctoral Thesis in Solid State Physics in 2018. She is associate professor at the Department of Photonics, Lviv Polytechnic National University. Authored over 150 publications. The area of her scientific interests includes plasmonics,

periodic structures, micro- and nanostructures, and optical elements on their base.

E-mail: iryna.y.yaremchuk@lpnu.ua



Yaroslav V. Bobitski, born in 1951, received both Ph.D degree in 1980 and Professor Habilitation in Technology of materials for electronic devices from the Lviv Polytechnic National University in 1991. Head of the Department of Photonics, Lviv Polytechnic National University.

Authored over 200 publications. The area of his scientific interests includes distribution light by nano-structured systems, interaction laser irradiation with layered media.